

WP PWIE Meeting 24-27 March 2025

# Analysis of changes in the surface and sub-surface structure of bulk tungsten lamellae and Langmuir probes operating under reactor conditions

E. Fortuna-Zalesna<sup>a</sup>, M. Spychalski<sup>a</sup>, W. Chrominski<sup>a</sup>, P. Wiecinski<sup>a</sup>, P. Petersson<sup>b</sup>, B. Thomas<sup>c</sup>, A. Widdowson<sup>c</sup>

<sup>a</sup>Warsaw University of Technology

<sup>b</sup>Royal Institute of Technology (KTH)

<sup>c</sup>UKAEA, Culham Campus, Abingdon









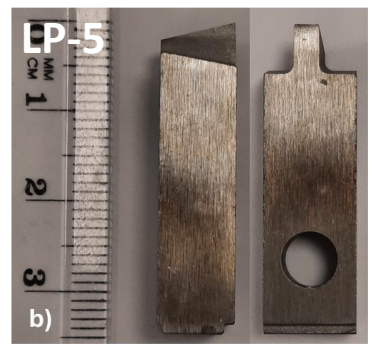


## Langmuir probes



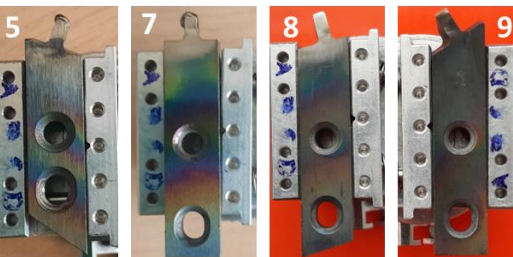
## **Experimental**





Langmuir probes arrays at Tile 5 and the appearance of LP-5.





#### **General Information**

#### **Examined samples:**

Langmuir probes 1, 3, and 5 from module 16W, Tile 5 (removed in 2015)

Langmuir probes 5, 7, 8, and 9 from module 16IN, Tile 3 (removed in 2015)

All JET Langmuir probes were manufactured via sintering and rolling with a tungsten purity greater than 99.95 %.

#### Task and questions to be addressed

The aim of the work was to (i) determine by nanoindentation the changes in mechanical properties of W components after long-term exposure in JET-ILW, (ii) assess surface and sub-surface modification of the material caused by the plasma—wall interactions (redeposition, recrystallization, melt damage, etc.).

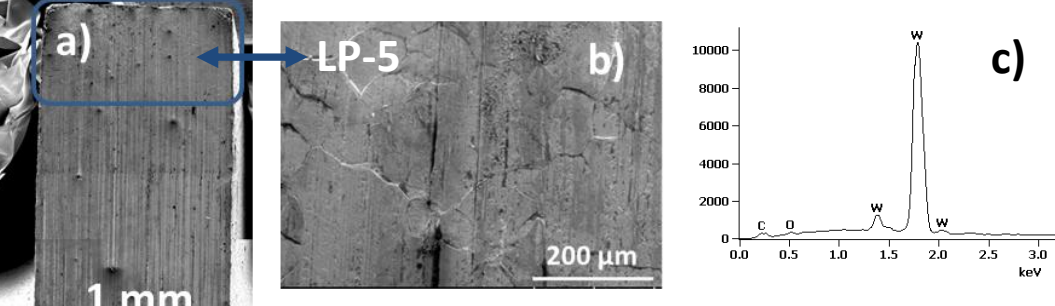
#### **Approach**

- Microscopic observations of the probe's surface along with studies of the chemical composition of the surfaces (SEM, EDX, IBA: ToF-HIERDA with a 44 MeV 127I<sup>8+</sup> beam)
- Nanoindentation (Hysitron Ti-900 triboindenter) Because of the small dimensions of the tip, the force applied was 10 mN; Due to the large development of the surface, it was imaged in the SPM mode before and after each measurement.
- FIB cross-sectioning to confirm possible recrystallization
- Optical profilometry
- XRD measurements

Scheme of the installation of the probes at Tile 3 and images of LP5, 7, 8, and 9.

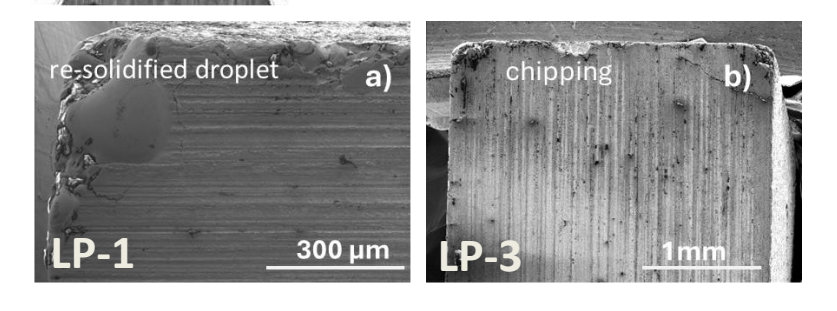


## Surface morphology – probes attached to Tile 5



#### SEM images of the probes' tips.

- No tip melt damage was observed for all probes.
- In the case of LP-5 large re-crystalized zone, ca. 1.3 mm with clearly visible GBs  $\sim$  100  $\mu$ m.
- Microscopic observation revealed some damage in the tip area of the other probes, but they were confined to the tip edge itself.



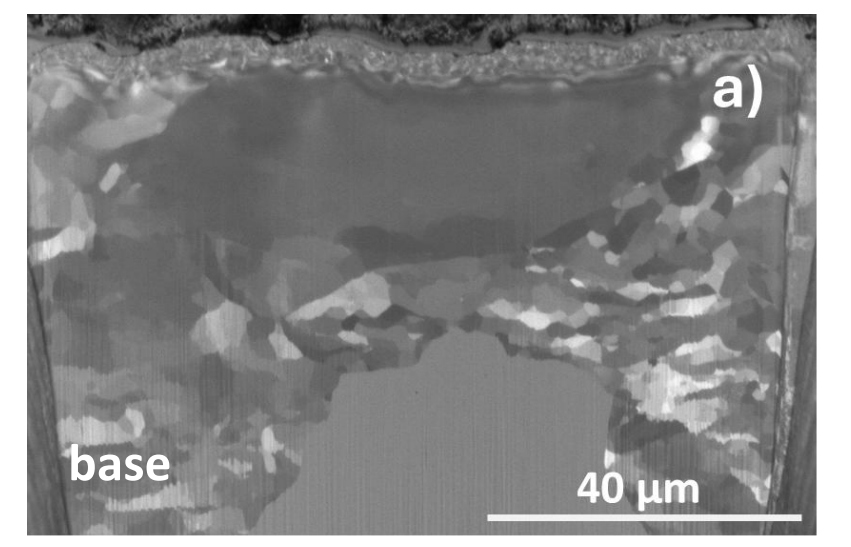
## 

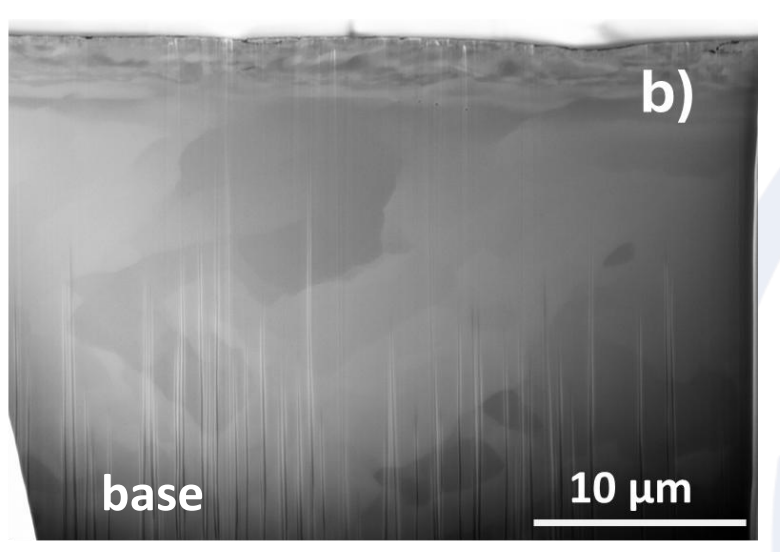
#### SEM images of the base morphology.

- No signs of re-melting.
- Re-deposit found at all four sides of the probes, in their middle and bottom parts, composed of oxygen, nitrogen, carbon, nickel and beryllium.
- Stronger redeposition in the surface grooves.



## **Sub-surface structure**



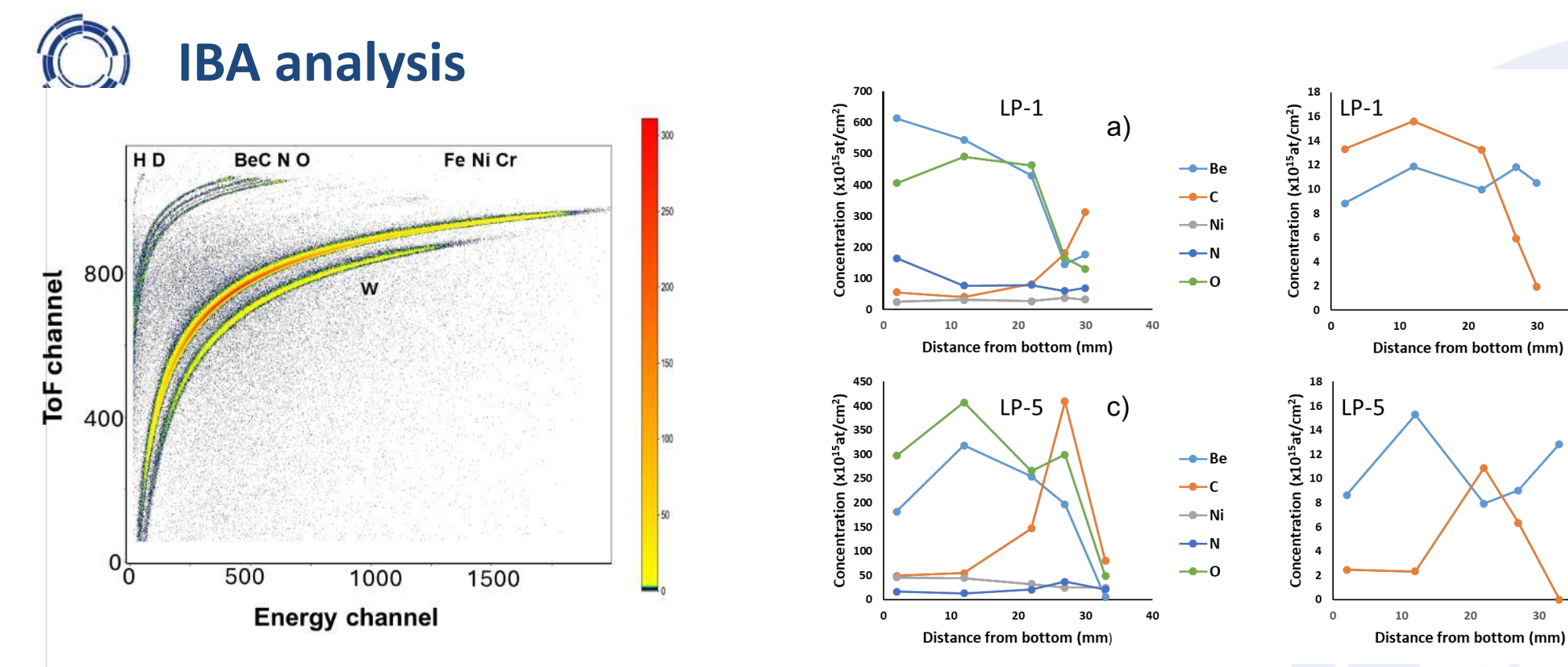


tip \_\_\_\_40 μm

FIB cross-sections of LP-5 base part: a) front and b) back side.

FIB cross-section of LP-5 tip, front side.

- A zone of plastic deformation with a thickness of ca. 3  $\mu$ m was revealed in the base part of the probe.
- The grains visible on the cross-sections made in the base part are approx. 10 μm in size.
- In the tip area equiaxed grains, with a size of the order of 40  $\mu$ m; a heavily deformed zone disappeared.



Results of the Langmuir probe analysis with ToF HIERDA

Distribution of deposit elements (a, c) and hydrogen isotopes (b, d) along the length of LP- 1 and LP-5, front side.

b)

d)

**--**1H

---2H

• Beryllium and oxygen are the main components of a thin film covering the probes' surface, along with carbon, an admixture of nickel, nitrogen puffed for plasma edge cooling, and hydrogen isotopes.

<sup>\*</sup>E. Fortuna-Zalesna et al. 2025 Fus. Eng. Des. 220 115319



### **Surface development**

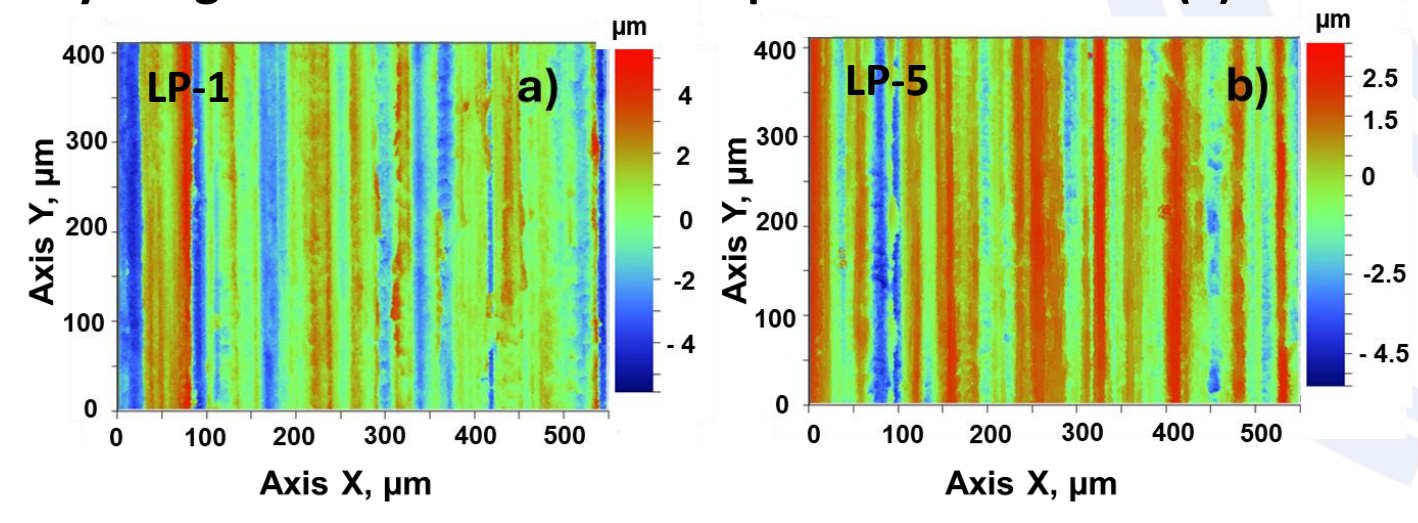
#### **Results of surface development measurements**

(mag. 11.5x, Ra was calculated from five areas with dimensions equal to  $412\times550~\mu\text{m}^2$ )

Roughness average, Ra [μm]										
Probe 1		Probe 3		Probe 5						
tip	base	tip	base	tip	base					
1.4 ± 0.2	1.3 ± 0.1	1.5 ± 0.1	1.4 ± 0.2	1.1 ± 0.1	1.0 ± 0.1					

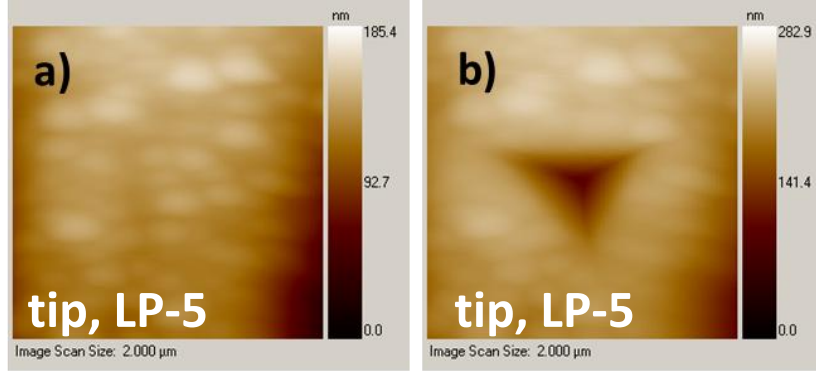
• Roughness values for the tip and the base for the examined probes are at the same level.

#### Exemplary images of the surface development in the base: (a) LP-1 and (b) LP-5.

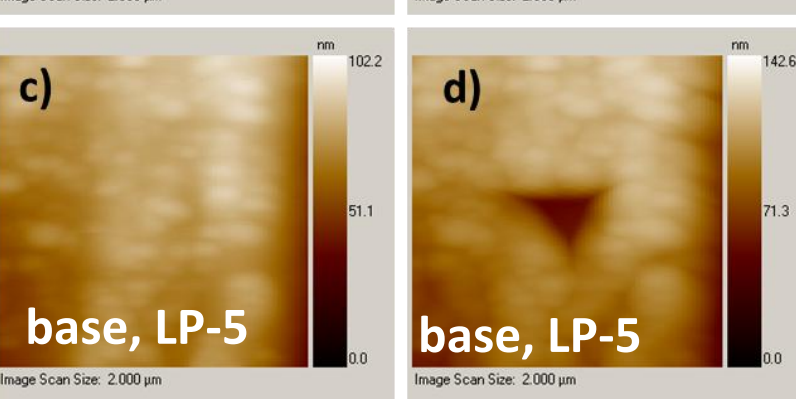




## Surface imaging in the SPM mode



SPM images of the probe surface before the measurement and of the imprint made on the recorded area, for the tip (a-b) and the base (c-d), LP-5, front side.



• The imprint from the tip area is larger and deeper.

Results of surface development measurements

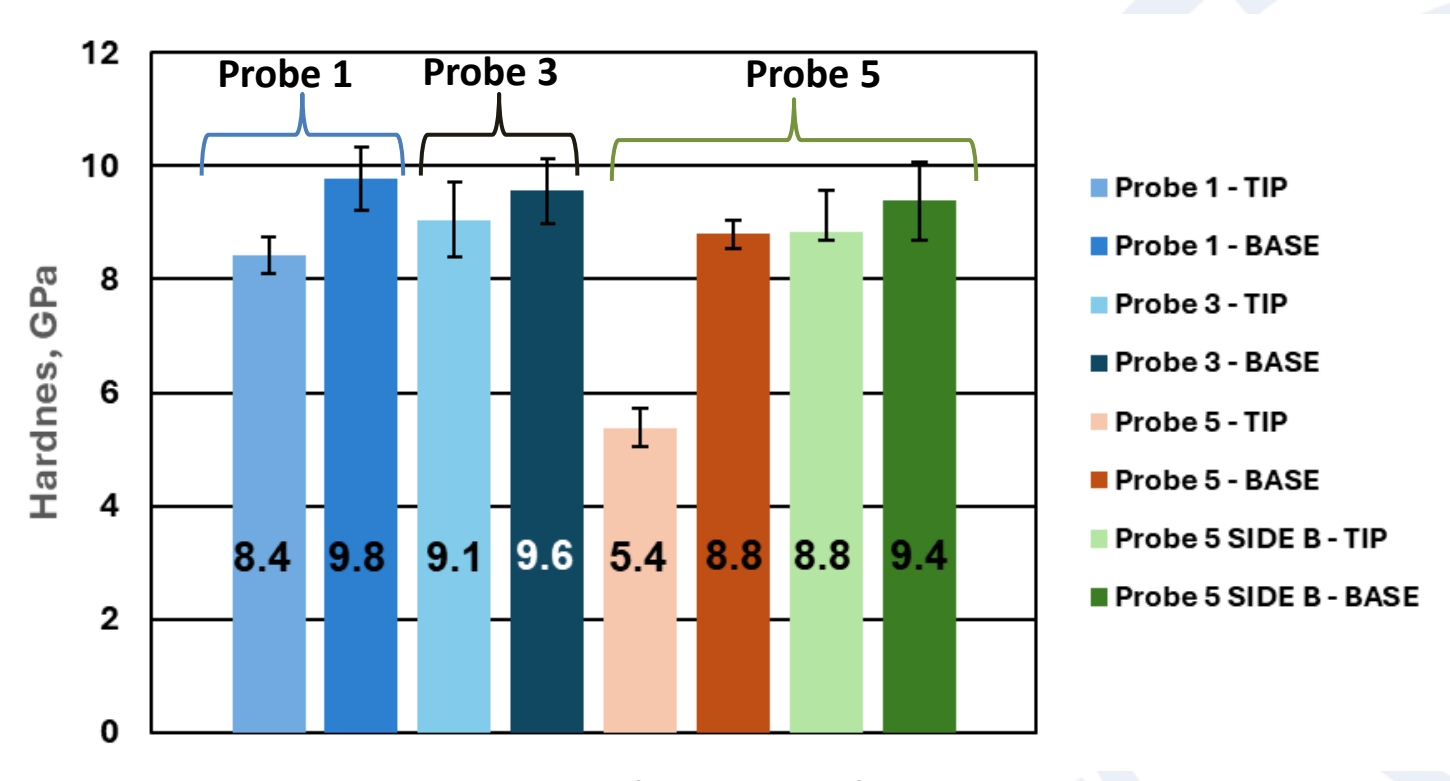
Roughness average, Ra [nm]											
Probe 1		Probe 3		Probe 5		Probe 5B*					
tip	base	tip	base	tip	base	tip	base				
14 ± 9	19 ± 3	15 ± 5	12 ± 6	13 ± 5	13 ± 3	11 ± 4	11 ± 4				

<sup>\*</sup>back side



## **Nanomechanical properties**

#### Results of nano-hardness measurements

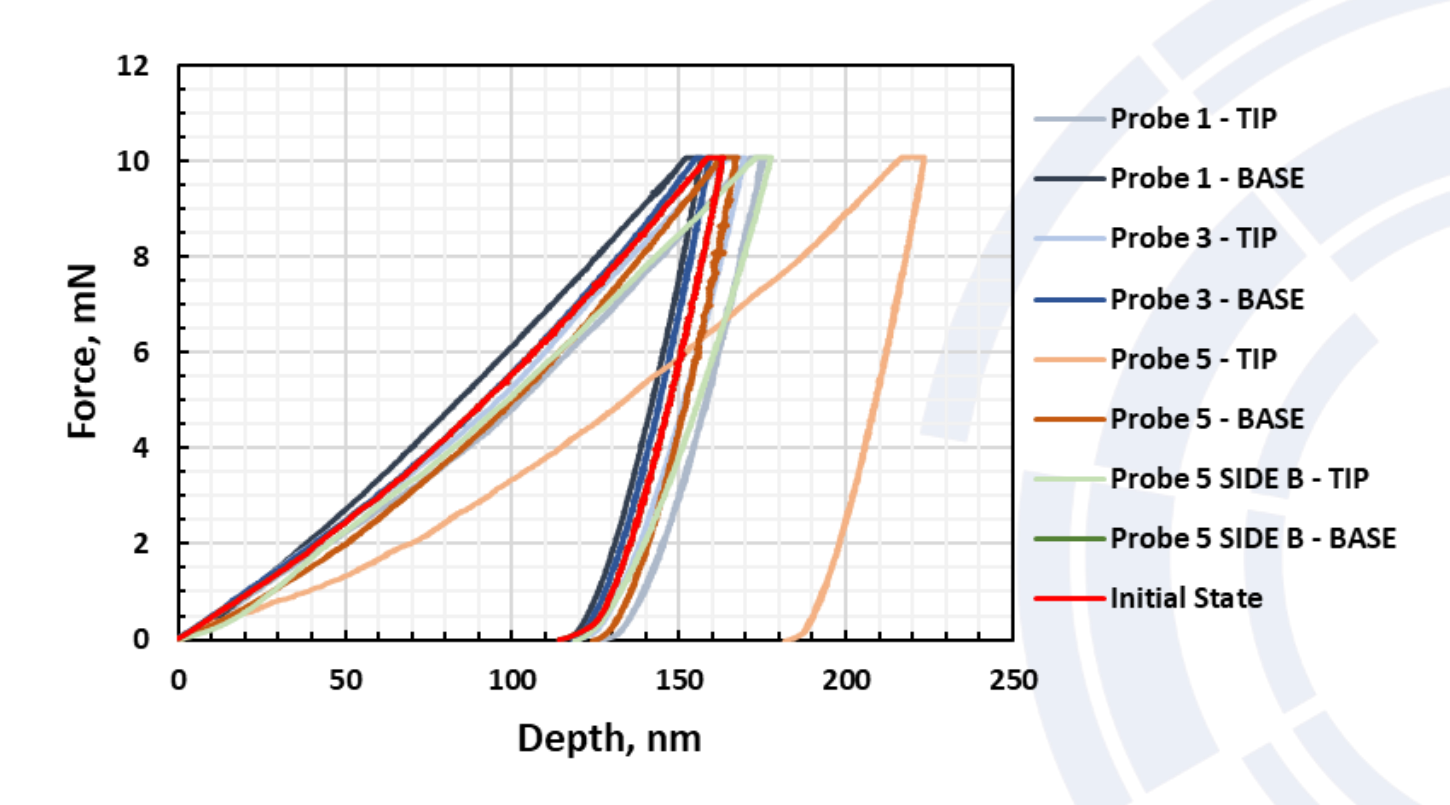


- Large difference in the hardness value in the tip and the base of LP-5 at the front side, 5.4 GPa versus 8.8 GPa, respectively.
- The differences in hardness on the base and tip of LP-1 and LP-3 are small, comparable to those obtained for LP-5 on the back side and its base part on the front side.

<sup>\*</sup>E. Fortuna-Zalesna et al. 2025 Fus. Eng. Des. 220 115319



## **Nanomechanical properties**



Comparison of force-depth curves for all examined zones

- The only curve that stands out from the others is the one obtained on the front side of the LP-5 tip.
- The results clearly document a high agreement in the mechanical properties of the single probes mounted in the divertor area.



- Nanoindentation carried out at room temperature provides adequate results for tracing the changes occurring in the subsurface zone of components made of tungsten. In combination with metallography and IBA analysis a broad insight into the metal PFC modification would be obtained.
- The results presented do not deviate from the literature data on tungsten. The nano-hardness at room temperature for recrystallized tungsten (with a mean grain size of 36  $\mu$ m) amounted to about 6.7 GPa compared to 8.4 GPa for the asforged state\*. Literature data for the tungsten nano-hardness found are in the range of 3.5-5.8 GPa for a recrystallized state.
- <u>The surface finish should be an issue that needs to be considered when procuring components for ITER</u>. This is important not only because of the potential recrystallization or damage formation. One should remember that the number of defects present in the material's structure can affect fuel retention. Additionally, the surface roughness influences the erosion rate.

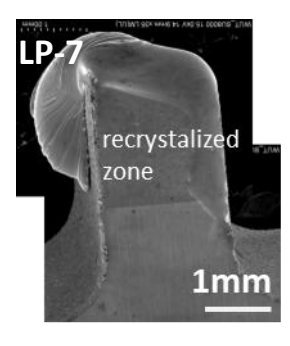
•

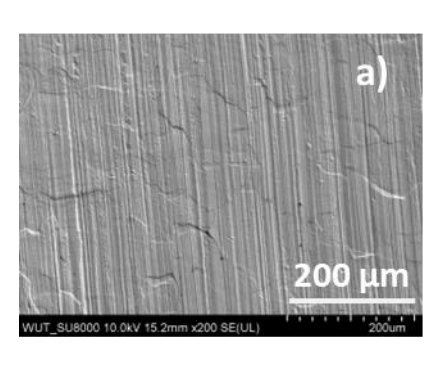
<sup>\*</sup>Terentyev D et al. International Journal of Refractory Metals & Hard Materials 89 (2020) 105222

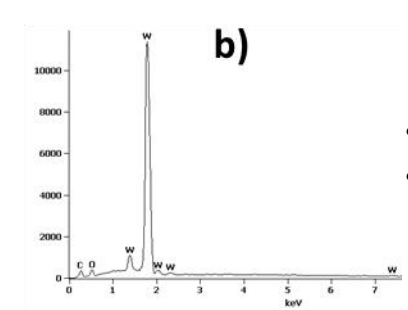


## Surface morphology – probes attached to Tile 3



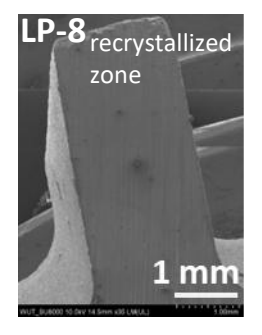


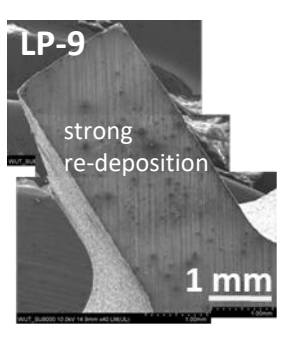


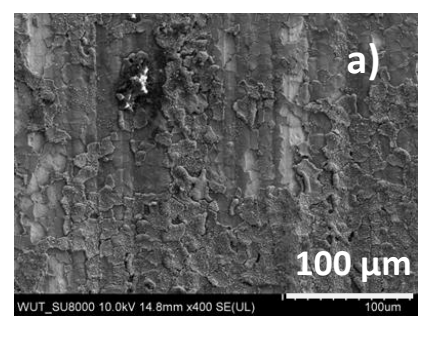


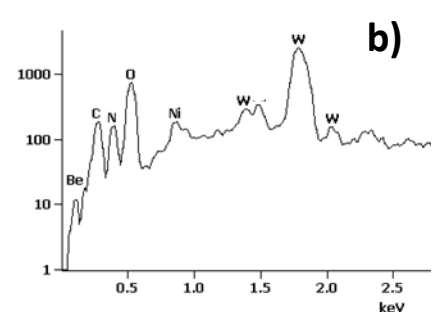
SEM image of the LP-7 tip morphology (a) together with (b) corresponding EDX spectrum, recrystallized zone.

- The melt damage of the tip edge observed on LP-5 and LP-7.
- Below this area recrystallized zone was present.

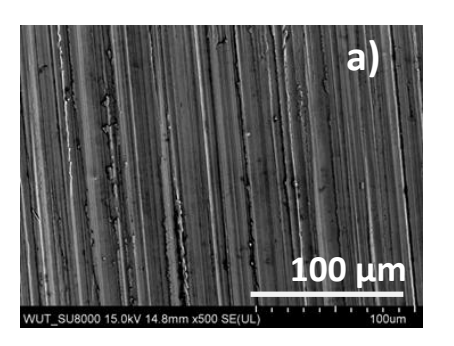


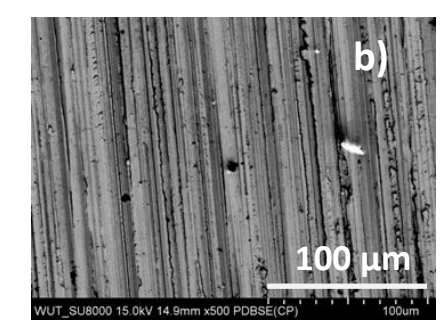


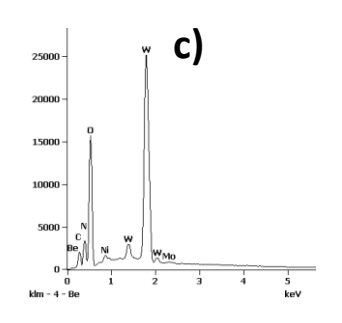


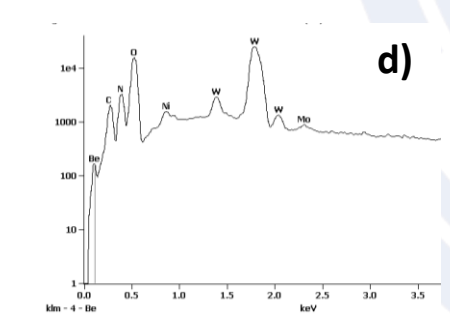


SEM image of the LP-9 tip morphology (a) together with (b) corresponding EDX spectrum.







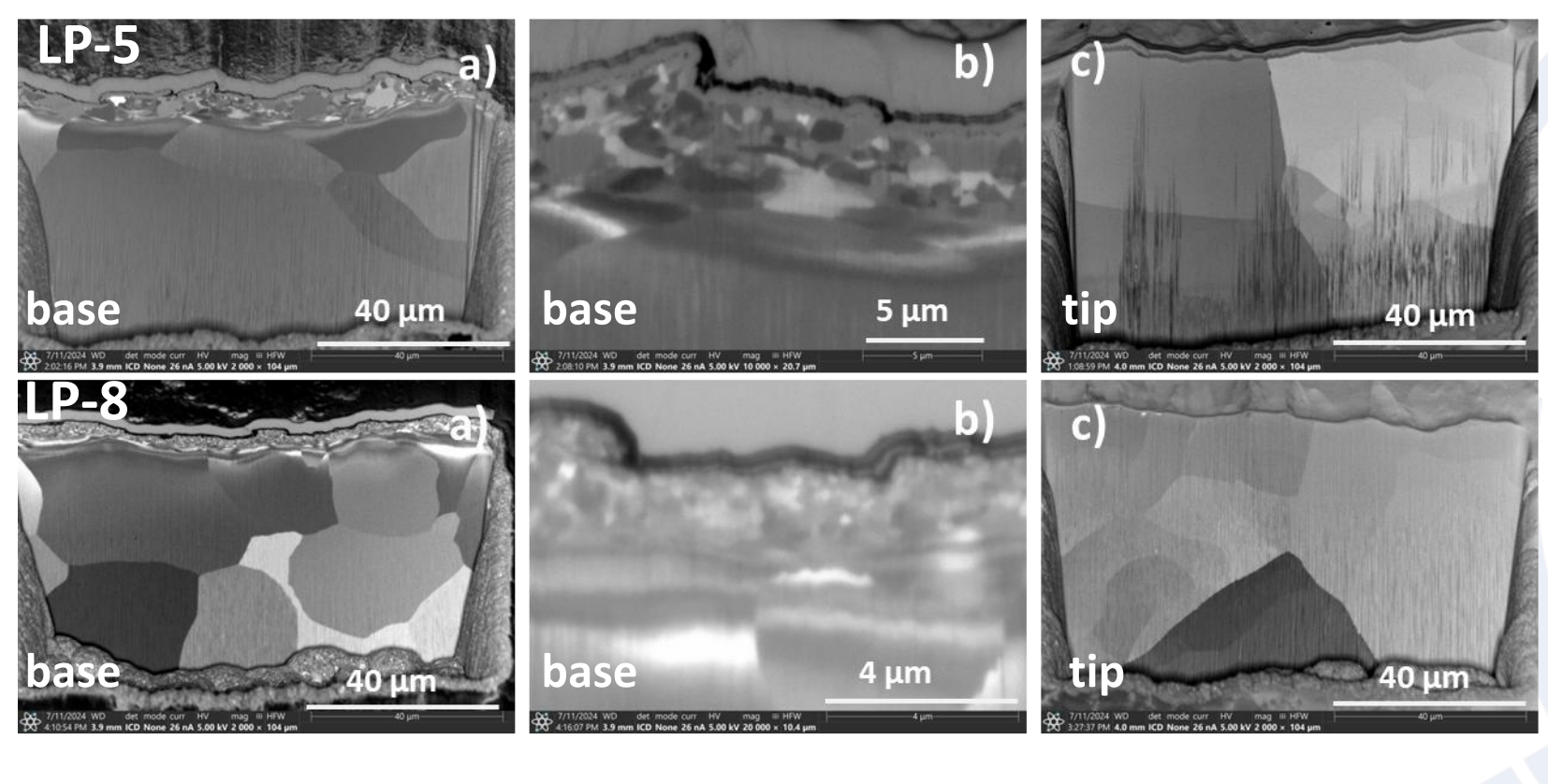


SEM image of the LP-7 base morphology (a-b) together with (c-d) corresponding EDX spectra

- The spectra recorded in the base and in the tip area are clearly different.
- In the area with the colored layer, the EDX spectra show lines originating from beryllium, oxygen, nitrogen, carbon, and nickel.



## **Probes sub-surface structure, FIB cross-sections**



SEM images of the sub-surface FIB crosssections taken in the base (a-b) and the tip (c) of probe LP-5.

SEM images of the sub-surface FIB cross-sections taken in the base (a-b) and the tip (c) of probe LP-8.

- A zone with fine grains near the surface is clearly visible, the so-called "surface deformation zone," observed in the base part.
- A stratified deposit found in the base part. The thickness of the deposit in the case of LP-5 can be estimated at around 0.6 μm.
- In the tip area, the surface deformation zone has disappeared, and the increase in the grain size is noticeable.



### Probes sub-surface structure, FIB cross-sections



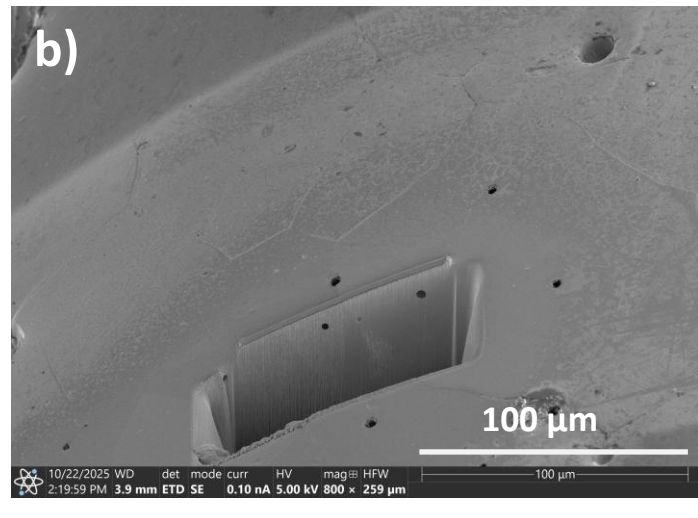
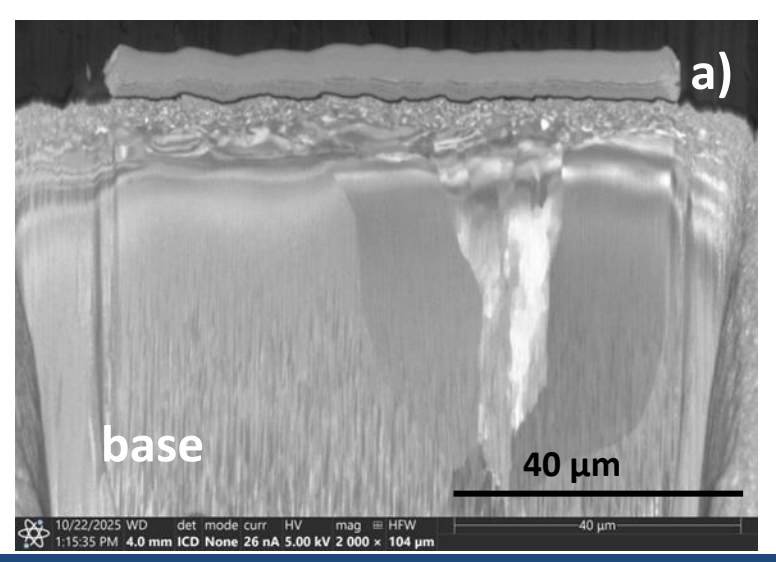


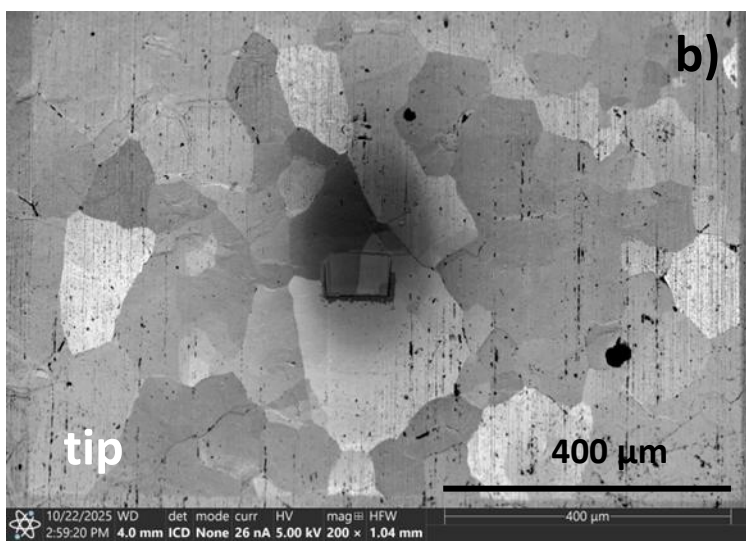
Image of LP7 (a) together with SEM image of the re-solidified zone present at the tip end (b).

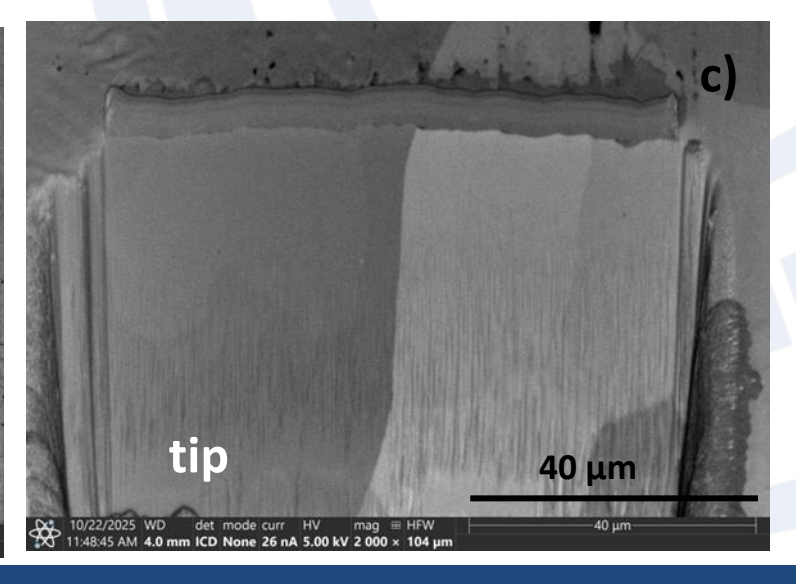
✓ Zone with distinct porosity.

FIB cross-sections of LP-7: a) base and (b-c) tip part (recrystalized zone).

- ✓ At the base surface, a zone of plastic deformation was revealed.
- ✓ A recrystallized zone was observed in the tip area.

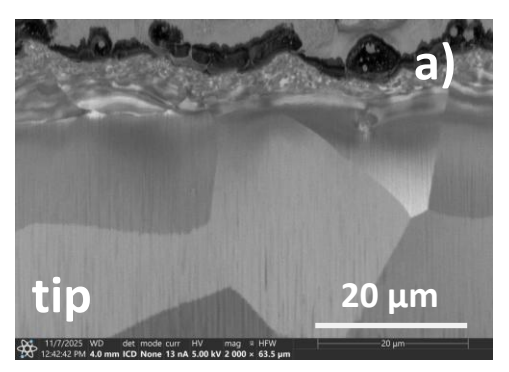


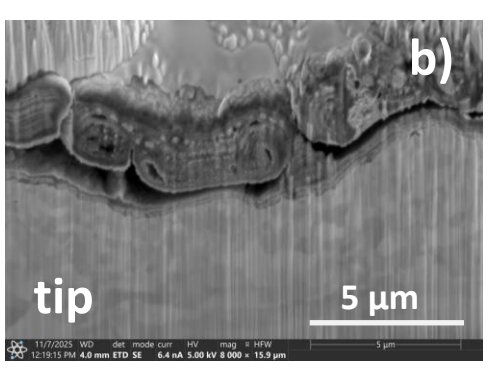


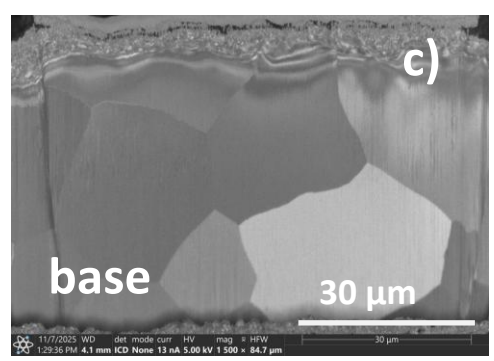


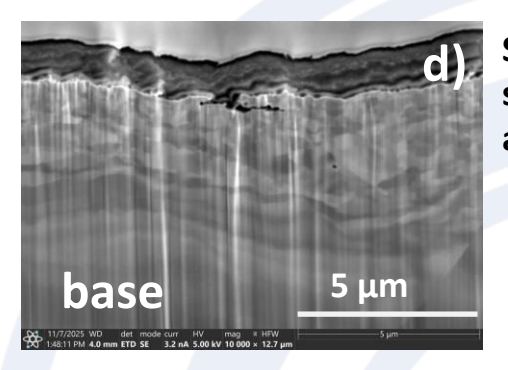


### Probes sub-surface structure, FIB cross-sections



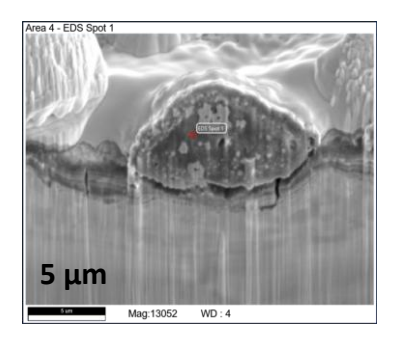


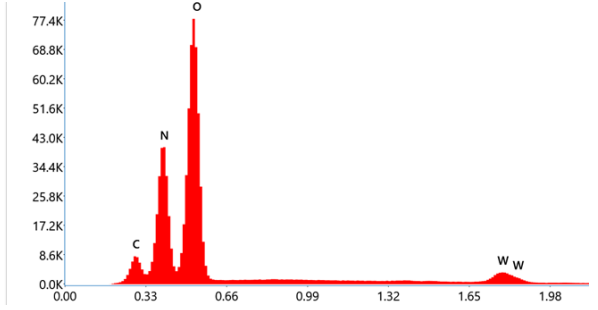


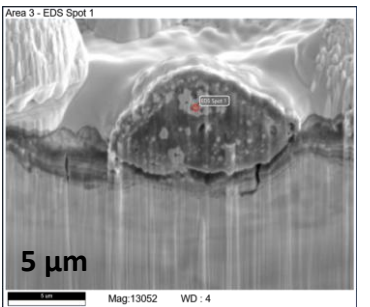


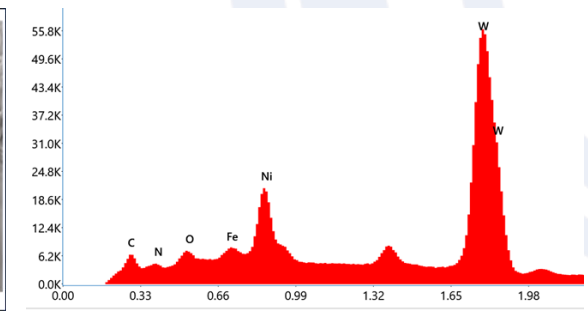
SEM images of the FIB crosssections taken in the base (a-b) and the tip (c-d) of probe LP-7.

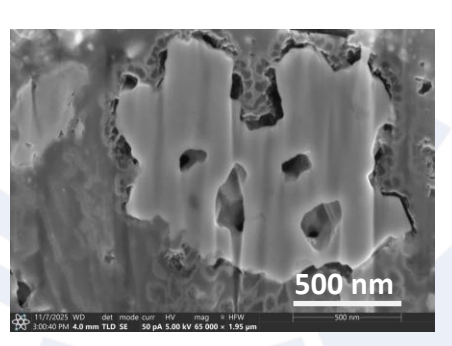
- A zone with fine grains near the surface is clearly visible in both zones.
- Grains of similar size are observed in both zones; no recrystallization takes place.
- Deposit present on both the base and the tip.











SEM images of the deposit together with EDS spectra, probe LP-7, tip.

The particles collected on adhesive carbon pads from Tile 6 after ILW-2 had a similar structure to that revealed on LP-7's tip, E. Fortuna-Zalesna et al. Nucl. Mat. Energy 12 (2017) 582)

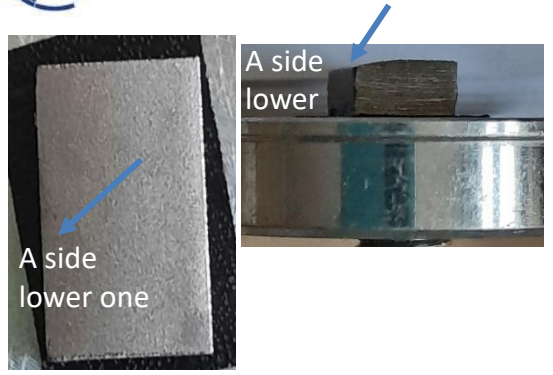


- The melt damage of the top part of the tip was observed on two of the four probes, namely LP-5 and LP-7. Below this area recrystallized zone was present. In the case of probe LP-8, the presence of a recrystallised zone was revealed at the tip end, in the absence of re-melting. A common feature of these three probes was a presence of a thin deposited layers on the base part of the probes. The tip and the base part just below it were clean, most likely due to plasma exposure.
- Microscopic observations confirmed the presence of re-deposit on the base part of the above-mentioned samples. The EDX spectra show it is composed of beryllium, oxygen, nitrogen, carbon, and nickel.
- Probe LP-9 stands apart from the others. On the tip of this probe, we observe neither melt damage nor a recrystallized zone, instead it is covered with a thick layer of redeposit, which is peeling and falling off in places.

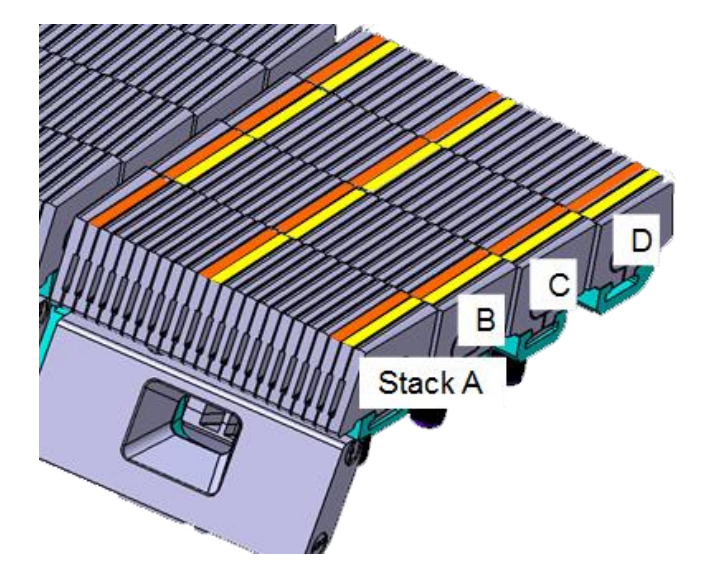


## W lamellae from divertor bulk tile 5





B12 (ILW1+3)
Dimensions 10 × 6 × 2.5 mm



**Bulk Tungsten Lamellae, Tile 5** 

#### **General Information**

#### **Examined samples:**

lamellae 157/B02 (ILW3) and 164/B12 (ILW1+3) from stack B of the bulk divertor Tile 5 lamella 106/C02 (ILW-3) from stack C of the bulk divertor Tile 5

#### Task and questions to be addressed

The aim of the work was to (i) determine possible lamella damage caused by plasma-wall interaction, (ii) assess surface modification of the material caused by the plasma-wall interactions, including redeposition, and (iii) assess sub-surface structure changes.

#### **Approach**

- On the sample, microscopic observations of the lamella surface, along with studies of the chemical composition of the surface and dust particles, were carried out (SEM/EDX).
- To characterize the near-surface zone, FIB cross-sections were made in areas with three characteristic morphologies: a) in surface depression, b) in convex, potentially re-melted areas, and c) through cracks.
- Thin foils were cut out from the lamellae 164 and 106 for TEM observation.
- The surface development was examined by the optical profilometer Veeco NT9300 at 3 magnifications of the device: 2.9, 11.5, and 28.4 x)



## Surface morphology, lamellae 157/B02

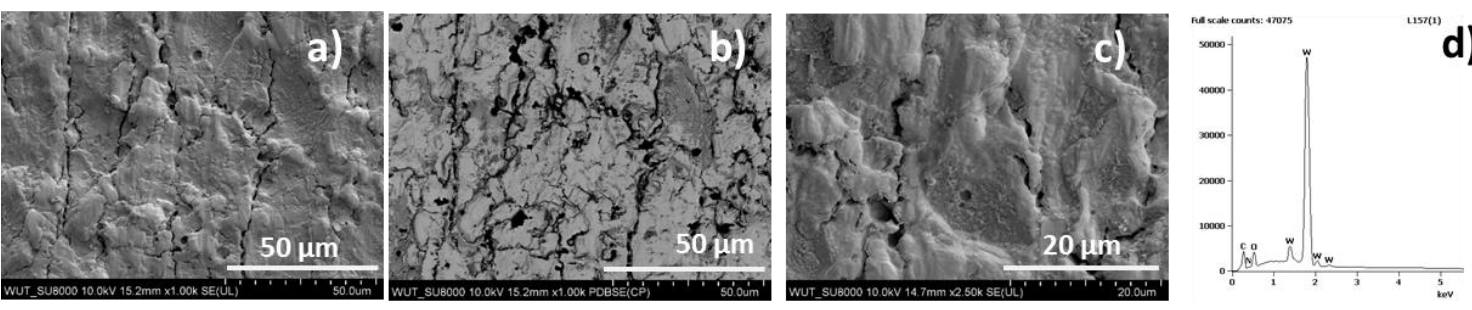


Fig. 1. SEM images of lamella 157 surface together with corresponding EDX spectrum from the area.

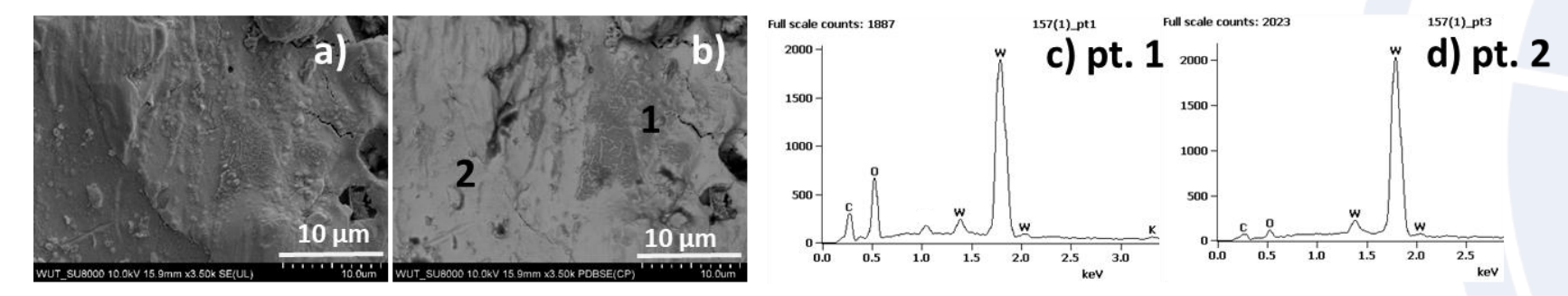


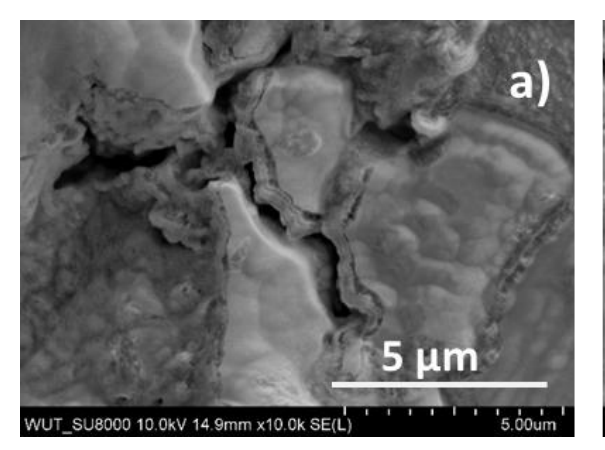
Fig. 2. SEM images of lamella 157 surface (a-b) together with corresponding EDX spectra (c-d).

Redeposition is visible in the images recorded in the BSE mode. EDX point measurements confirm higher levels of C and O in the darker contrast areas.

- Highly developed surface. On the entire surface, there are longitudinal cracks, regular with constant intervals, ca. 40 μm, in addition, a
  network of finer cracks is visible on the surface.
- Visible traces of surface remelting. Pores present.
- Locally, at the edges, a changed structure (re-deposit, traces of re-melting).
- In the EDX spectrum, the increased signal from C and O. N is present.
- Such a morphology is a result of the manufacturing process (the last step: electrical discharge machining (EDM)).
- Based on the research, it is impossible to clearly determine which damage occurred at the material production stage and during operation.



### Lamella 157



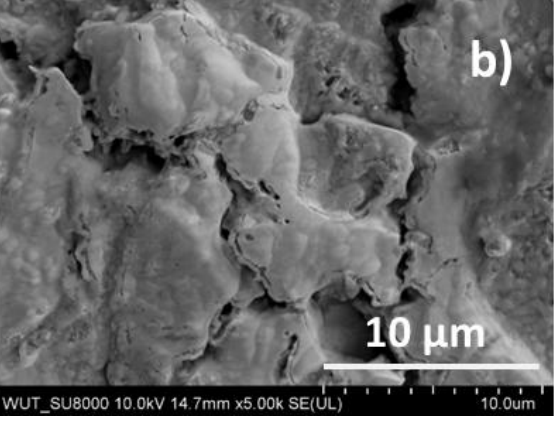


#### Fig. 1. SEM images of lamella 157 surface.

- ✓ Redeposition inside the cracks, locally in the cavities and on edges (shadowed areas).
- ✓ In these areas, we observe material with a different, porous, or stratified structure, sometimes with traces of re-melting.
- ✓ EDX point measurements confirm higher levels of O and C, locally also N, Ni, and Fe in these areas.

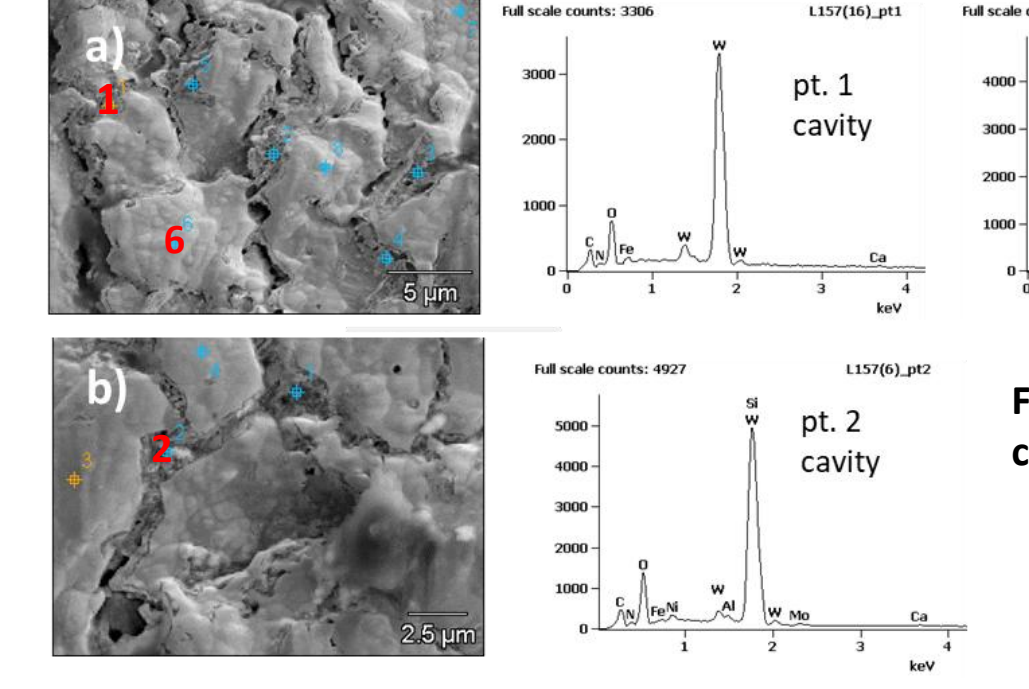


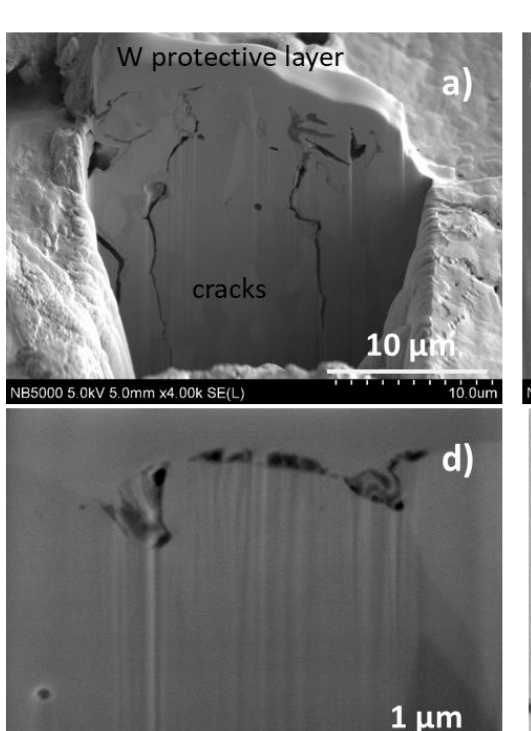
Fig. 2. SEM images of lamella 157 surface along with the corresponding EDX spectra.

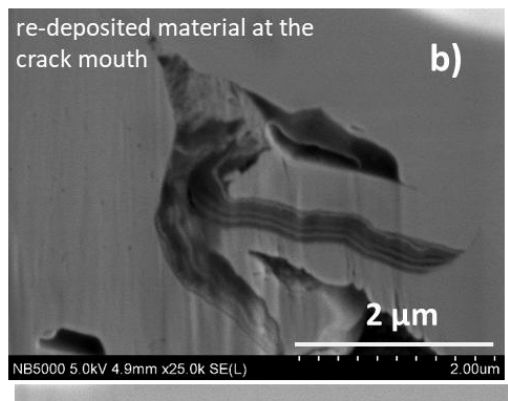
pt. 6

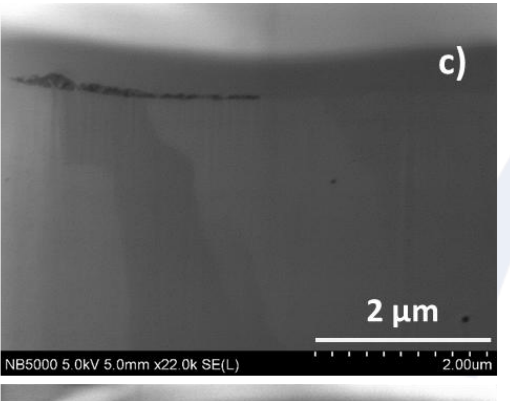
surface

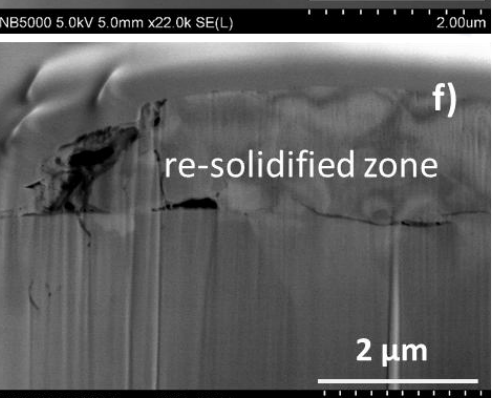


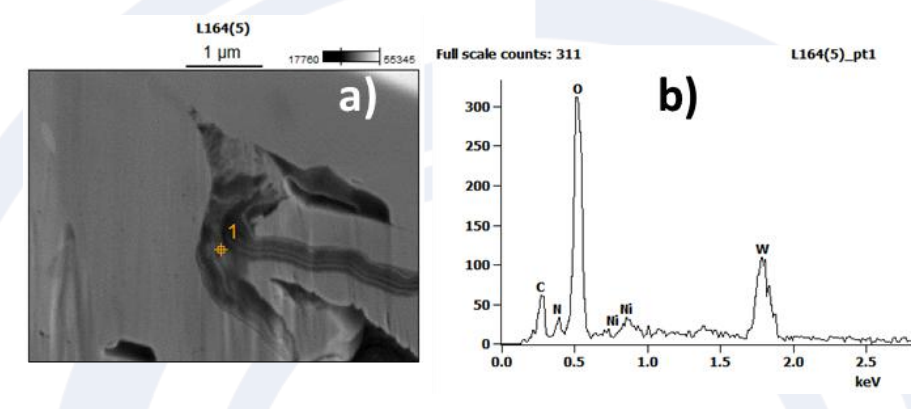
## Lamellae 157/B02 and 164/B12 – FIB cross-sections observations









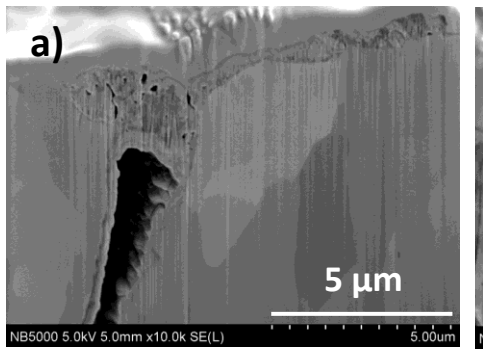


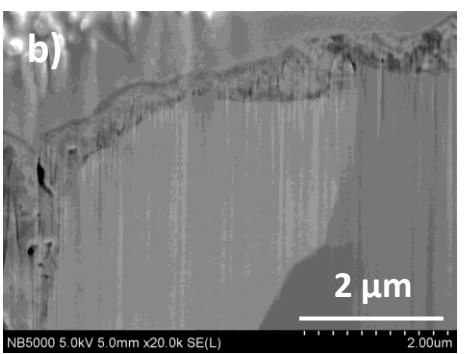
- At the crack mouths, the presence of a material with a different chemical composition than the substrate, Figs. a-b.
- The presence of a thin film of redeposit has been locally revealed, Figs. c-d.
- A zone with changed morphology (likely re-solidified) was observed in some places, Figs. e-f.
- In Fig. e, a structure with a different, porous morphology is shown, Fig. e.
- In the case of sections made in the cavities, the material was almost unchanged, as far as can be determined using the FIB technique.

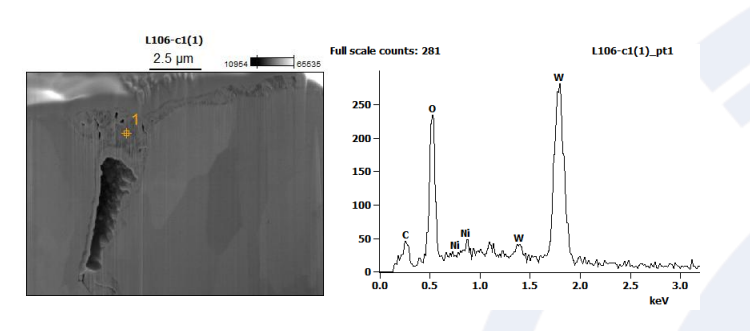
porous

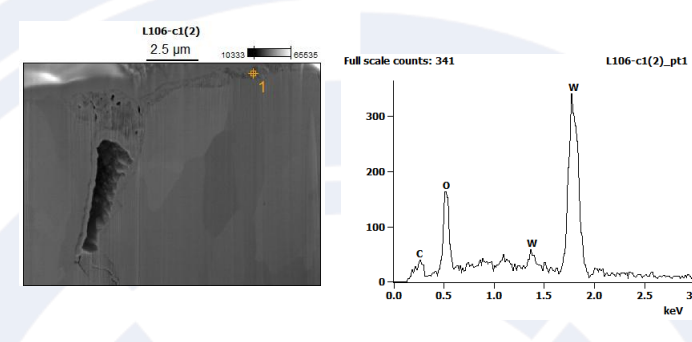


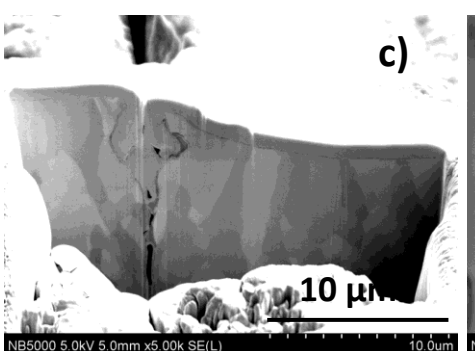
## Lamella 106/C02 – FIB cross-sections observations

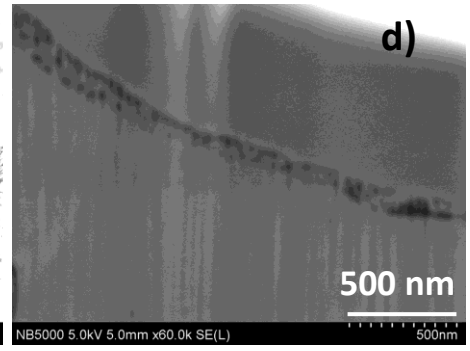


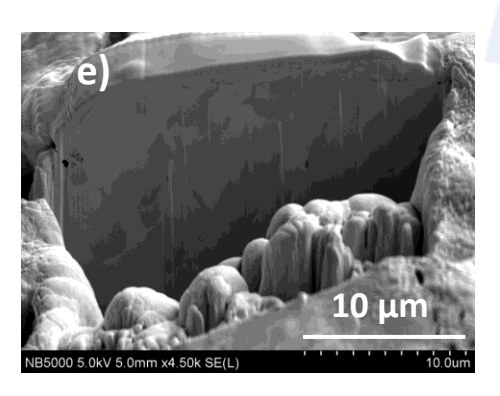


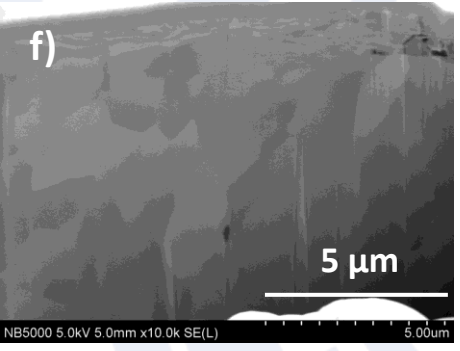










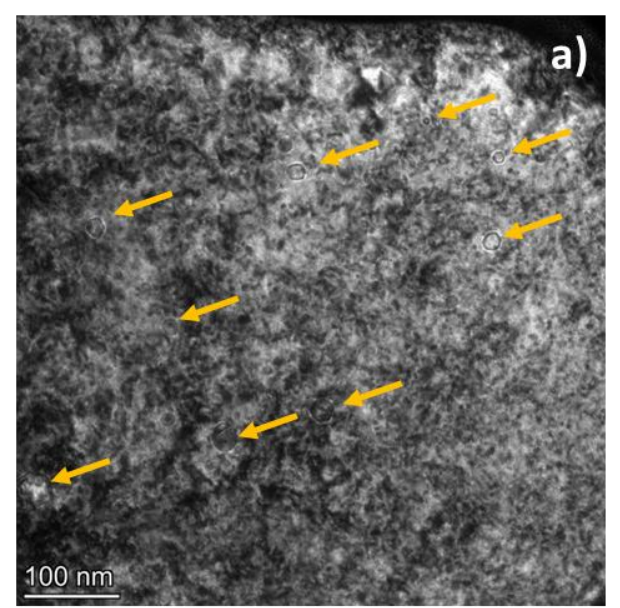


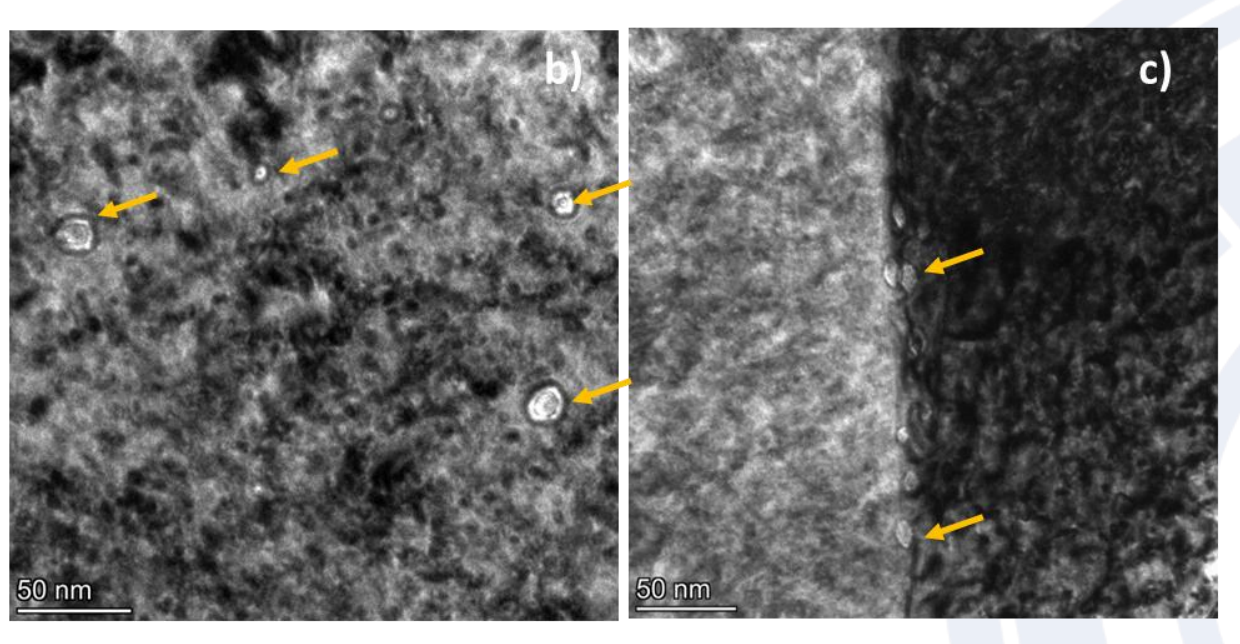
SEM images of lamella 106 FIB cross-sections.

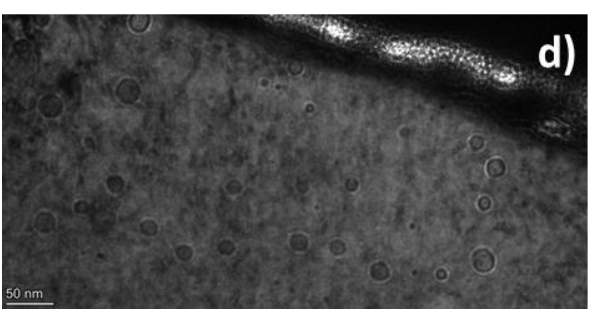
- At the crack mouths, the material with a different chemical composition than the substrate present, Figs. a,c.
- The presence of a thin film of redeposit has been locally revealed (in surface cavities), Figs. a-d. The deposit shown in Figs. a and b is relatively thick (0.8 μm) and porous, with no layering distinguishable. The deposit revealed in Fig. d is much thinner, around 170 nm.
- A zone with changed morphology (likely re-solidified) was locally observed Figs. e-f.



## Lamella 164/B12 – TEM examinations bubbles





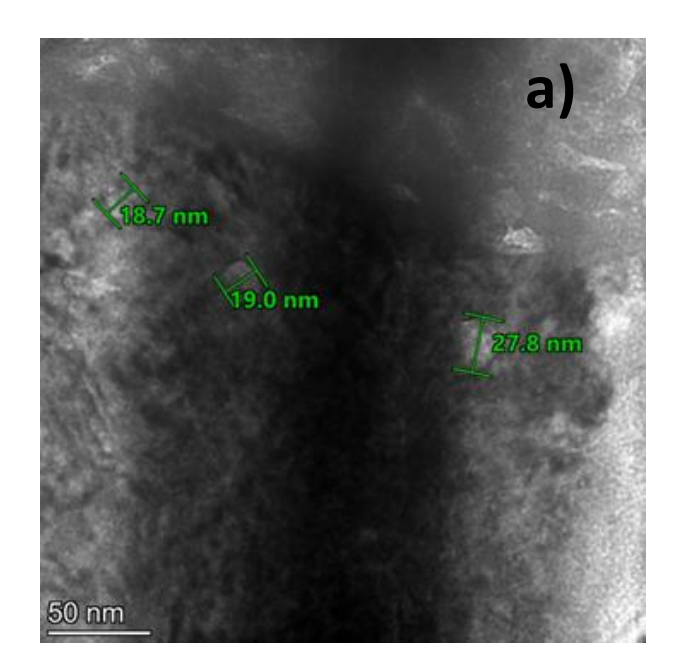


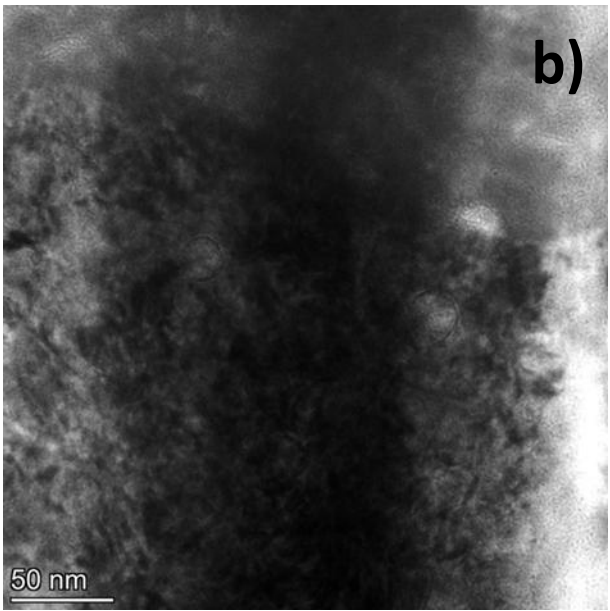
#### TEM images of bubbles present in the subsurface zone of 164 lamella.

- ✓ The bubbles (10-30 nm in diameter) populate the region over 500 nm in depth. They are also present at the grain boundaries.
- ✓ The size and distribution of the bubbles are consistent with what Tokitani observed at not-exposed lamella (Phys. Scr. T171 014010).
- ✓ Those bubbles are considered to be formed during the manufacturing process.



## Lamella 106/C02 – TEM examinations bubbles





#### TEM images of bubbles present in the subsurface zone of 106 lamella.

Single bubbles (20-30 nm in diameter) found in the near-surface zone of the sample.



## Lamella 164/B12 – re-deposits

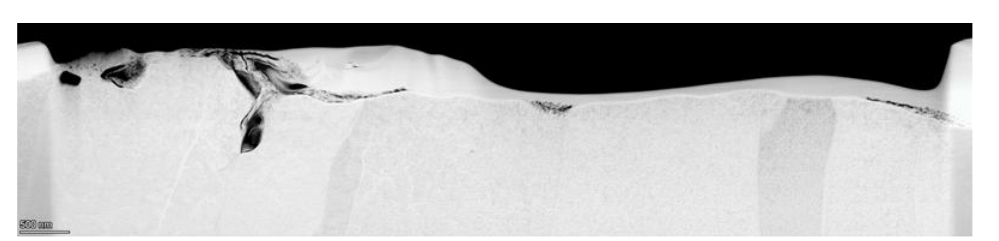


Fig. 1. STEM images of thin foil cut out from lamella 164.

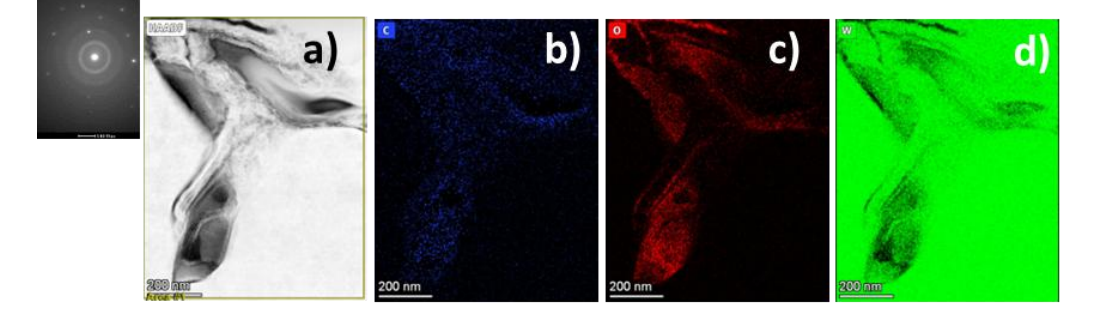


Fig. 2. STEM image of redeposit present in the crack mouth and mapping of O, C, and W inside re-deposit

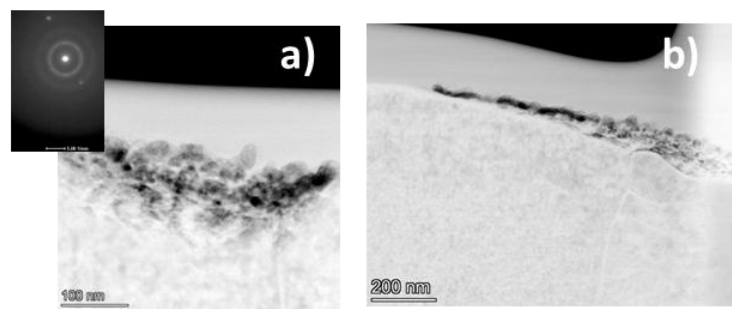


Fig.3. STEM image of granular redeposit present in the surface cavities.

- ✓ The re-deposited material in the crack mouth has a partly porous and layered structure, Fig. 2.
- ✓ On the right side of Fig. 1 there are two areas with granular re-deposits, Fig. 3. Both are located in depressions present on the surface. Thickness 130 and 100 nm, respectively. Both have an amorphic structure and are characterized by increased C and O content.



Au protective layer

## Lamella 106/C02 – re-deposits

Au protective layer

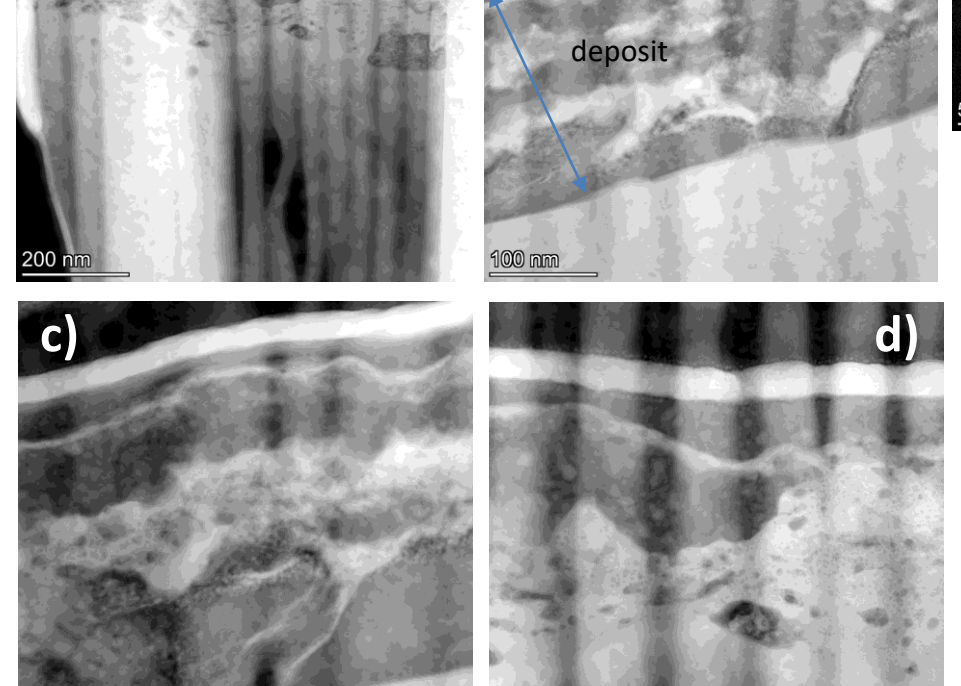
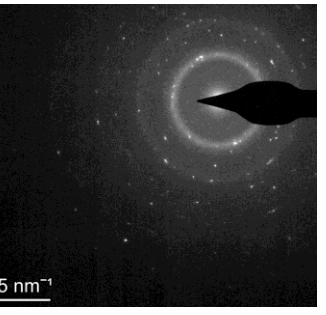


Fig. 1. STEM images of redeposit present at the surface.



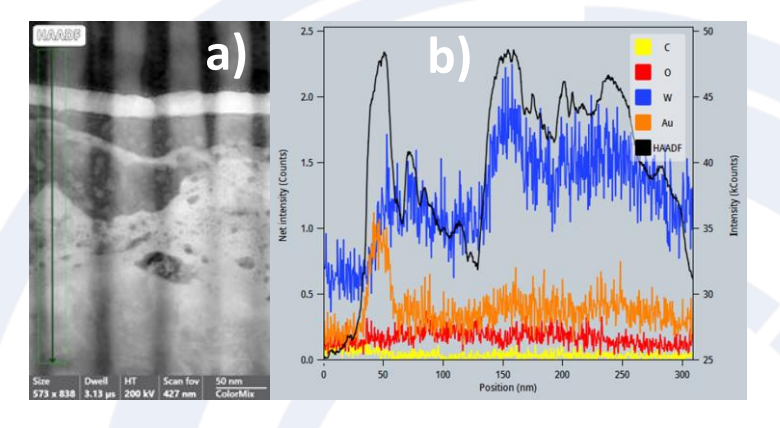
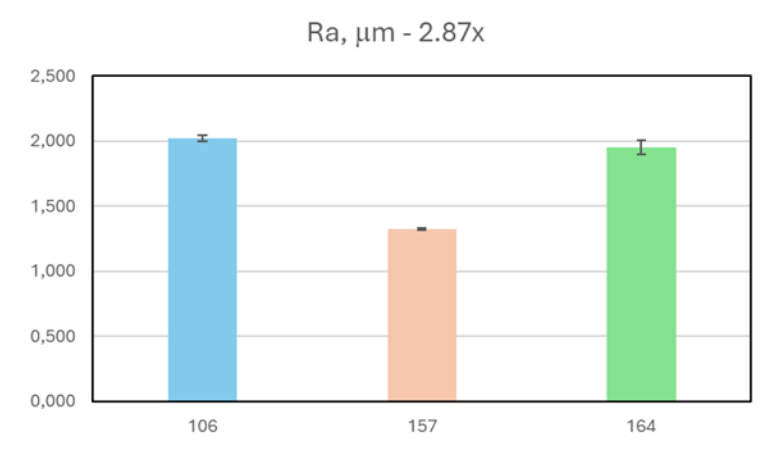


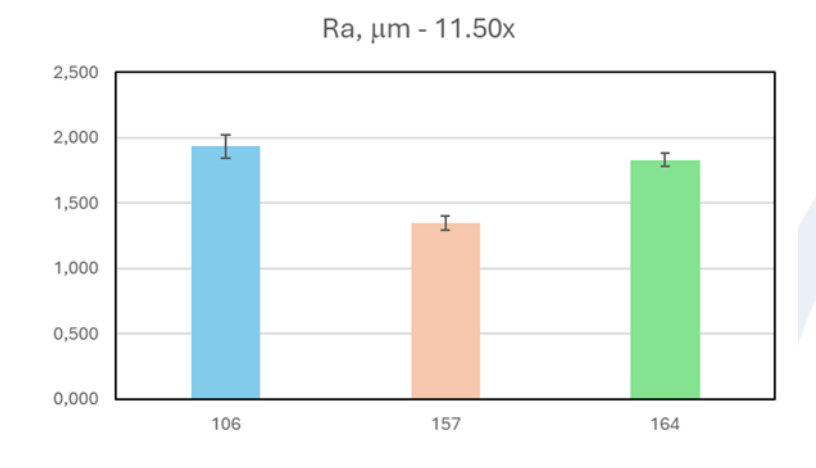
Fig. 2. STEM image of redeposit with the place of measurement marked (a) and the line scans of C, O, W, Au, and intensity distribution for STEM image (b).

- On the surface there is an amorphous, inhomogeneous, porous deposit ~200nm thick.
- Within the deposit there are areas of varying chemical composition, as evidenced by differences in image contrast.
- The intensity distribution can be related to the tungsten content. In the area where linear EDX analysis was carried out, a higher tungsten content was found at the substrate boundary.

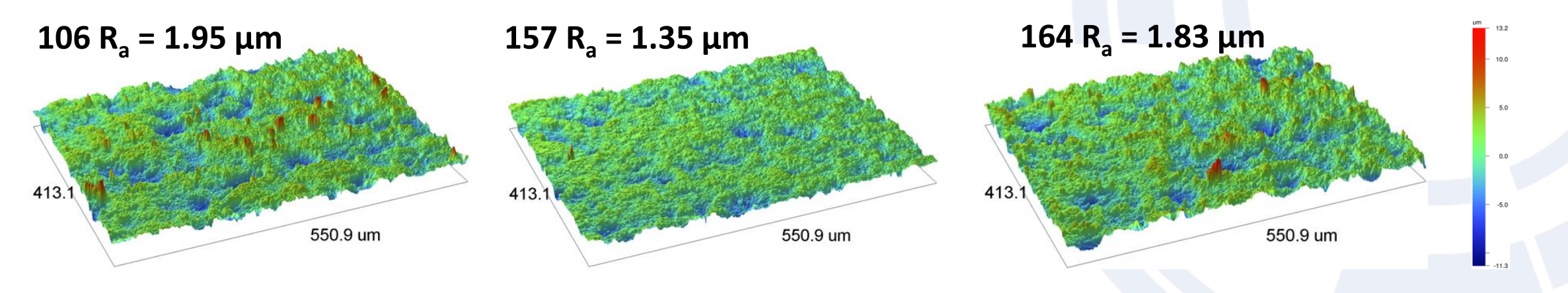


### **Roughness measurements**





Bar charts showing differences in roughness between samples.



The recorded 3D maps confirm that sample 157 has lower roughness. The differences in height between the lowest and highest areas are noticeably smaller (mag. 11.5x).



- On the entire surface, there are longitudinal cracks, regular with constant intervals, ca. 40 µm. In addition to a grid of major longitudinal cracks running through the whole sample, a network of finer cracks is visible on the surface.
- Visible traces of surface remelting. Pores are present, often located along the cracks.
- Redeposition is visible in the images recorded in the BSE mode. EDX point measurements confirm higher O levels in the darker contrast areas.
- Redeposition is observed inside the cracks, locally in the cavities, and on edges (shadowed areas). Sections carried out
  through the cracks revealed the presence of a material with a different chemical composition than the substrate at the
  mouth of the cracks and in the crack itself. EDX measurements showed that the material had a high oxygen and elevated
  carbon content. Locally, nickel was found to be present. In the surface cavities, the thickness of the deposit reached 0.8 μm.
- TEM observations revealed the presence at the surface of an amorphous, inhomogeneous, porous deposit ~200nm thick.



## Literature regarding Langmuir probes and W lamellae

#### Langmuir probes

- ✓ E. Fortuna-Zalesna et al. 2025 Fus. Eng. Des. 220 115319
- ✓ M. Spychalski et al 2021 Phys. Scr. 96 124072
- ✓ R. Kerr et al 2023 NME 35101420

#### W lamellae

- ✓ G. Pinchuk et al 2020 Phys. Scr. 96 T171 014042
- ✓ M. Tokitani et al 2020 Phys. Scr. T171 014010
- ✓ E. Fortuna-Zalesna et al 2021 Phys. Scr. 96 124038
- ✓ M. Tokitani et al 2024 NME 39 101678
- ✓ R. Kerr et al 2024 IEEE TRANSACTIONS ON PLASMA SCIENCE, VOL. 52, 4054



## Thank you for your attention